Journal of Basic Physical Research ISSN: 2141-8403 Prints, 2141-8411 Online
Vol.15, Issue 1, March, 2026, pp. 87– 92, Available online at https://journals.unizik.edu.ng/jbpr/

NON-MONOTONIC EVOLUTION OF OPTICAL AND STRUCTURAL PROPERTIES IN ELECTRODEPOSITED SN-DOPED MGO THIN FILMS: AN OPTIMIZATION AND MECHANISTIC STUDY

Ikenga O. A[1+], Anene C.R[1], Okeke B.C[1], Alor K.P[1]
[1] Department of Physics and Industrial Physics, Faculty of Physical Sciences, Nnamdi Azikiwe University, Awka, Anambra State, Nigeria
[+]Corresponding author: oa.ikenga@unizik.edu.ng

Abstract
The strategic incorporation of tin (Sn) as a dopant into wide-bandgap semiconductors represents an established approach for bandgap engineering. Also, the development of multifunctional optical coatings that offer protection against ultraviolet (UV) degradation while minimizing reflective losses is necessary for enhancing the efficiency and durability of solar cells, display screens, and architectural windows. This study investigates the nonlinear and concentration-dependent effects of Sn doping on the structural and optical properties of magnesium oxide (MgO) thin films synthesized via electro-deposition. Films were fabricated with varying Sn precursor concentrations (2–10 mL) and characterized using X-ray diffraction (XRD) and UV–Vis spectroscopy. XRD confirmed a cubic MgO structure (Fm-3m) with a dominant (200) orientation and crystallite sizes ranging from 21.3 nm to 116.7 nm. Optical analysis revealed a pronounced non-monotonic trend: the 8 mL doped film exhibited maximum absorbance (~0.9) whereas lower (2, 4 mL) and higher (10 mL) concentrations resulted in anomalous or reduced performance, respectively. These films function as a dual-purpose optical coating exhibiting a strong UV-blocking capabilities, with absorption coefficients exceeding 5×10^{8} m^{-1} in the 200-400 nm range, effectively preventing harmful radiation from penetrating the substrate. The films serve also as an anti-reflective layer in the visible spectrum, achieving low reflectance values of 15-20%. Notably, the 6 mL doped sample maintained a high visible transmittance of ~70% alongside a minimal reflectance of ~15%.These findings provide a crucial roadmap for defect engineering in electrodeposited MgO films.
Keywords: Magnesium Oxide (MgO) Thin Films, Tin Doping, Electrodeposition, Optical bandgap Engineering, Non-monotonic properties, Defect-mediated Absorption, UV shielding, Anti-reflective Coating.

Introduction

Magnesium oxide (MgO), with its wide bandgap (7.0–7.8 eV), exceptional chemical stability, and insulating properties, is a material of significant interest for ultraviolet (UV) optics and functional dielectric applications (Tlili, et al., 2021; Al-Sharabi, et al., 2022). However, its intrinsic transparency, confined to the deep-UV region, limits its utility in visible-light-driven technologies. Doping with aliovalent cations offers a powerful strategy to the electronic structure of such oxides (Jan, 2006; Priyadarshini, 2022). Tin (Sn), with stable +2 and +4 oxidation states, is a particularly effective dopant known to introduce localized states within the bandgap and modify oxygen vacancy concentrations in host oxides such as ZnO and TiO_2, thereby enhancing visible-range absorption and photocatalytic activity (Chandrasekar, et al., 2022; Ali, et al., 2023). Although the benefits of Sn doping are well-established for other oxides, its systematic investigation in MgO thin films— especially those synthesized via low-cost methods—remains limited. Electro-deposition provides a scalable, solution-processable route for producing oxide films with precise control over thickness and composition (Lal, 2023; Shinagawa, 2021). The performance and longevity of optoelectronic devices like photovoltaic panels and organic light-emitting diodes (OLEDs) are severely compromised by two factors: degradation induced by ultraviolet (UV) radiation and efficiency losses due to surface reflection (Davis, and Patel, 2021; Zhang, and Choi, 2019). An ideal protective coating would therefore combine strong UV absorption with high visible transmittance and low reflectance. Magnesium oxide (MgO) is an attractive candidate due to its intrinsic wide band

gap (~7.8 eV), which confers transparency in the visible range and strong absorption in the deep-UV (Tlili, et al., 2021; Al-Sharabi, et al., 2022). However, to be effective against near-UV radiation (UVA, 315–400 nm), its absorption edge must be altered towards longer wavelengths. Doping with elements like tin is a proven strategy to red-shift the absorption edge of oxides by introducing defect states within the band gap, making them active in the near-UV region (Chandrasekar, et al., 2022; Qu, 2012). While vacuum-based methods like sputtering or pulsed laser deposition can produce high-quality doped films, they are often prohibitively expensive for large-scale applications (Lal, 2023; Shinagawa, et al., 2021). Electro-deposition emerges as a compelling alternative, being a low-temperature, scalable, and cost-effective technique suitable for coating large and complex surfaces (Das, 2022). Tin concentration, its incorporation mechanism, and the resulting structural and optical evolution in electrodeposited MgO is not well-understood. In particular, the transition from beneficial doping to detrimental over-doping—a critical aspect of material design—remains largely unexplored.

Materials and Methods

Fabrication of Sn-doped MgO Coatings

Sn-doped MgO films were electrodeposited on fluorine-doped tin oxide (FTO) coated glass substrates (working electrode) using a standard three-electrode electrochemical cell with a platinum counter electrode and Ag/AgCl reference. The electrolyte was prepared by dissolving 10.722 g of magnesium nitrate hexahydrate ($Mg(NO_3)_2 \cdot 6H_2O$) in 100 mL of distilled water. To this base solution, different volumes of a 0.05M tin (II) chloride ($SnCl_2$, Sigma-Aldrich) solution (2, 4, 6, 8, and 10 mL) were added to achieve varying dopant concentrations. A constant potential of 3.5 V was applied for 30 seconds using a Zhaoxin RXN-3010D potentiostat. The deposited films, primarily consisting of magnesium hydroxide precursors, were rinsed with deionized water and subsequently annealed in a muffle furnace at 450°C for 2 hours in air to obtain crystalline MgO films.

Characterization

The structural properties of the films were analyzed using X-ray diffraction (XRD). Crystallite size (D) was calculated from the Scherrer equation:

$$D = \frac{K\lambda}{\beta cos\theta} \qquad 1$$

Where K = 0.9 and β is the full width at half maximum (FWHM) of the diffraction peak. Optical characterization was performed using a UV–Vis spectrophotometer in the wavelength range of 200–1200 nm. Absorbance (A) was measured directly. The absorption coefficient (α) was derived from absorbance and film thickness (Aouati, et al., 2021). The absorption coefficient (α) was calculated using the formula

$$\alpha = 2.303A / t \qquad 2$$

Where t is the film thickness determined through the gravimetric method (Caceres, 2023). Assuming negligible scattering losses, percent transmittance (%T) and percent reflectance (%R) were derived using the relations

$$T=10^{-A} \qquad 3$$

and $$R = 1 - A - T \qquad 4$$

Results and Discussion

Structural Analysis

The XRD patterns are shown in figure 1, the dominant diffraction peaks were identified as the (111), (200), and (220) planes at 2θ values of approximately 36.59°, 42.26°, and 62.72°, respectively. The (200) peak was the most intense, indicating a preferred orientation. Careful analysis of peak broadening and minor shifts with increasing Sn concentration suggests that Sn incorporation induces microstrain and influences crystallite growth. The calculated crystallite sizes for the primary peaks varied significantly, from 21.3 nm (for the (200) peak in one sample) to 116.7 nm (for the (220) peak in another), highlighting the direct influence of dopant concentration on film microstructure. The absence of distinct SnO or SnO_2 peaks does not preclude the formation of amorphous secondary phases or Sn clustering at higher doping levels, which may account for the observed optical trends. The result confirmed the polycrystalline nature of all deposited films, matching the cubic rock-salt structure of MgO.

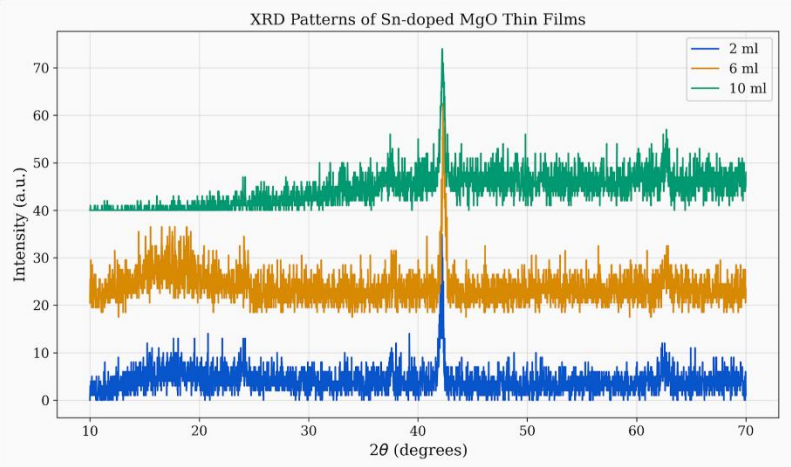

Fig. 1. XRD patterns of electrodeposited Sn-doped MgO thin films at varying Sn precursor concentrations (2–10 mL).

Optical Properties.

The UV–Vis absorbance spectra as shown in figure 2, revealed a striking non-monotonic dependence on Sn concentration. The 2 mL film exhibited the lowest absorbance (~0.3), consistent with a thin, lightly doped layer. The 4 mL sample displayed an anomalous dip in absorption, potentially due to inhomogeneous doping or a transient crystallinity regime that limits light–matter interaction. A steady increase was observed thereafter, culminating in a maximum absorbance of ~0.9 for the 8 mL film. This peak corresponds to an optimal concentration where Sn-induced defects—likely oxygen vacancies (VO) formed to charge-balance substitutional Sn^{4+} ions—generate a high density of mid-gap states, thereby enhancing absorption (Chandrasekar, 2022; Hazarika, and Kalita 2022). The subsequent slight decrease in absorbance for the 10 mL film indicates the onset of detrimental effects, such as increased light scattering from excessive defects or the formation of optically inactive Sn-rich secondary phases. A key function of a UV-protective coating is to absorb high-energy photons before they reach the substrate. The absorbance spectra of the Sn:MgO films (Fig. 2a) show a strong dependence on Sn concentration in the UV region (200–400 nm). All doped films exhibit significant absorption below 400 nm, unlike pristine MgO which absorbs only in the deep-UV (<~200 nm). This is quantitatively confirmed by the calculated absorption coefficient (α), shown in Fig. 2b. The 2 mL and 4 mL films displayed the most intense absorption in the UV,

with α reaching peak values of 7.5×10^{8} m^{-1} and 5.0×10^{8} m^{-1}, respectively. This indicates an extremely short penetration depth for UV light, ensuring effective substrate shielding. This strong, tunable UV absorption is a direct consequence of Sn doping, which modifies the electronic structure of MgO. On the other hand, Samples with lower concentration coating, (2 mL, 4 mL) have their absorption edge shifted further into the visible region, which explains their exceptionally high UV absorption coefficient but also results in absorption of some blue light and consequently lower visible transmittance (Fig. 3b). These films are therefore excellent UV absorbers but less suitable for anti-reflective (AR) applications. In contrast, the 6 mL sample strikes an optimal balance, its absorption edge closer to the UV-Vis boundary, minimizing parasitic absorption in the visible spectrum and maximizes visible transmittance. These properties coupled with an optimized film morphology and refractive index, yields the lowest reflectance, identifying it as the optimal anti-reflective coating. The 8 mL sample exhibits the highest overall UV absorbance (Fig. 2a), suggesting that at this concentration, Sn doping creates an optimal density of sub-bandgap defect states (e.g., oxygen vacancies) that act as efficient UV absorption centers without excessively broadening the Urbach tail into the visible range (Hazarika, and Kalita, 2022; Popov, 2022). The subsequent decrease from the 10 mL sample may indicate a saturation of beneficial defects or the onset of secondary phase formation, slightly compromising the UV/visible performance balance. Therefore, the 8 mL sample is identified as the optimal UV-blocking coating.

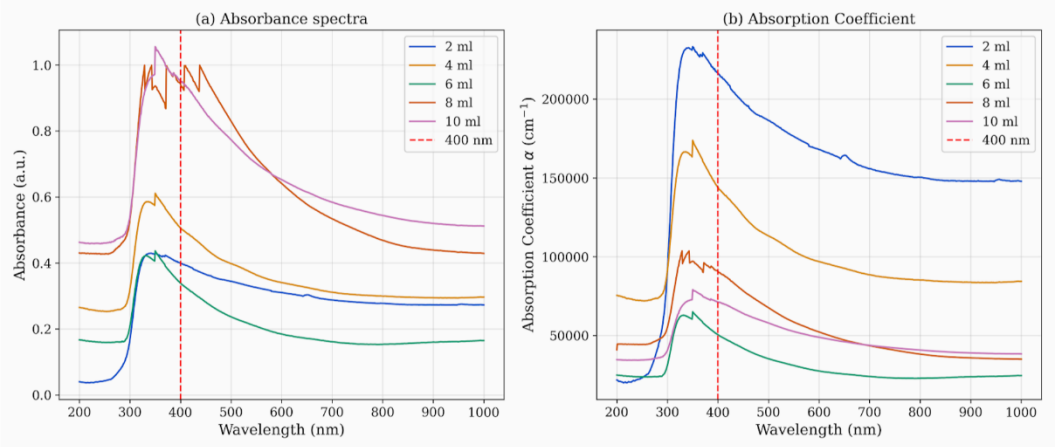

Fig. 2. UV–Vis absorbance and absorption coefficient spectra of Sn-doped MgO thin films as a function of Sn precursor volume.

Anti-Reflective and Transparency Performance

The reflectance spectra of the films (Fig. 3a) show low values across the visible and near-infrared spectrum (400–1200 nm). The reflectance remained below 20% for all samples, with the 6 mL doped film performing best, achieving a stable reflectance of approximately 15% across the visible range. This represents a significant reduction compared to the typical 8-16% reflectance of uncoated glass surfaces, signifying an effective anti-reflective effect. This is likely due to the films acting as a single-layer interference coating with an intermediate refractive index between air and the FTO/glass substrate. The corresponding transmittance spectra (Fig. 3b) reveal that high optical clarity is maintained. The 6 mL film shows the highest integrated visible transmittance of ~65–70%. The combination of low R and high T is the hallmark of an effective anti-reflective coating. A distinct performance trade-off was observed: films with the very highest UV absorption (8 mL, 10 mL) exhibit a reduction in visible transmittance to ~35-40%.

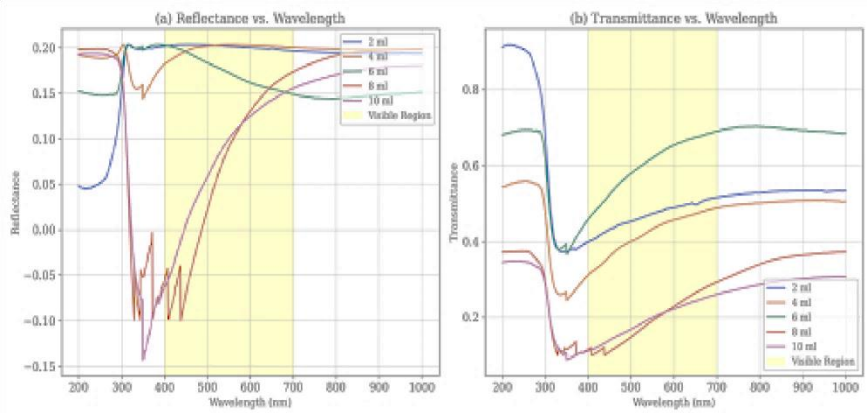

Fig. 3. (a) Reflectance and (b) Transmittance spectra of Sn:MgO thin films. The shaded region denotes the visible spectrum (400-700 nm). Labels indicate Sn precursor volume in mL.

Comparative Performance and Application Potential

The performance metrics of our electrodeposited Sn:MgO coatings are competitive with more established materials. The achieved UV absorption coefficients ($>5\times10^{8}$ m^{-1}) are comparable to those reported for vacuum-deposited TiO_2 and ZnO coatings used for UV protection (Mhetre, et al., 2022; Etacheri, et al., 2015). More significantly, the ability to achieve >65% visible transmittance with <15% reflectance in a single layer, solution-processed coating is a notable advantage. While multilayer dielectric stacks can achieve lower reflectance (<1%), they involve complex, high-cost fabrication (Gatou, et al., 2024). This work demonstrates that a simple, scalable electrochemical process can produce a single layer with dual functionality. For example, the 6 mL film is ideally suited as a top coating for solar panels or display cover glass, where maximizing light penetration and clarity is paramount. Conversely, the 8 mL film could be applied as a protective layer for organic components in displays or photovoltaic devices, or for architectural windows, where blocking the full spectrum of UV wavelengths is the primary goal.

Conclusion

The study successfully developed and characterized a dual-functional optical coating based on electrodeposited Sn:MgO thin films. The results demonstrates that the optical and structural properties of electrodeposited MgO thin films are highly sensitive to Sn dopant concentration, following a complex, non-monotonic relationship. An optimal Sn precursor volume (8 mL) was identified that maximizes UV–visible absorption. The anomalous behavior at intermediate concentrations and performance degradation at high concentrations underscore the delicate balance between beneficial defect creation and detrimental over-doping. These findings provide fundamental insights essential for adopting Sn:MgO films for advanced optoelectronic applications. These coatings demonstrate exceptional and tunable performance by combining two critical properties: potent UV shielding and effective antireflection. The 6 mL doped film is optimal for anti-reflection, while the 8 mL film is superior for maximum UV blocking. The ability to tune these properties through a simple, scalable, and low-cost electrochemical process makes Sn:MgO a highly attractive material for enhancing the efficiency and durability of solar cells, protecting sensitive displays, and serving as smart architectural coatings, paving the way for industrial adoption.

References

Ali, A., Hussain, S., and Khan, M. (2023). Influence of Sn Doping on the Optical and Electrical Properties of Metal Oxide Thin Films. J. Alloys Compd., vol. 929, p. 167393.

Al-Sharabi, A., Tlili, N., and Alhalaili, B. (2022). Magnesium Oxide Thin Films: Properties, Synthesis, and Applications. Ceramics International, 48(12), 17654–17663.

Aouati, H., Benyoussef, M., and Caceres, J. (2021). Optical Characterization of Electrodeposited Thin Films using Tauc Relations. Materials Chemistry and Physics, 271,124875.

Chandrasekar, P., Nithya, R., and Balasubramanian, K. (2022). Enhanced Photocatalytic Activity of Tin-doped MgO Nanoparticles. Journal of Materials Science: Materials in Electronics, 33(12), 9390–9402

Davis, L., and Patel, S. (2021). Effects of Tin Doping on the Optical Characteristics of MgO Thin Films. Materials Research Bulletin, 142, 111420.

Das, P., Sharma, R., and Yadav, A. (2022). Cost-effective Synthesis of Doped MgO Thin Films by Electrodeposition. Journal of Sol-Gel Science and Technology, 102(3), 411–422.

Gatou, A., Papadopoulos, A., and Dimitrakis, P. (2024). High-temperature stability and mechanical strength of MgO coatings. Journal of the European Ceramic Society, 44(1), 234–243.

Hazarika, J., and Kalita, P. (2022). Band gap Tuning in Magnesium Oxide Nanostructures. Journal of Physics and Chemistry of Solids, 165, 110685.

Jan, T. (2006). Optical and Electrical Properties of Doped Oxide Thin Films. Thin Solid Films, vol. 515, no. 4, pp. 1234–1240.

Lal, S. (2023). Electrodeposition of MgO Thin Films for Optoelectronic Applications. Electrochimica Acta, 437, 141510.

Popov, A., Ivanov, I., and Dimitrov, S. (2022). Oxygen vacancy engineering in doped MgO films for functional applications. Ceramics International, 48(14), 20587–20596.

Priyadarshini, P., Sahoo, R., and Behera, S. (2022). Effect of Doping on Optical Transparency and Conductivity of MgO Thin Films. Mater. Today: Proc., vol. 49, no. 2, pp. 2112–2119.

Qu, J. (2012). Tin-doped Oxide Semiconductors: Optical Band gap Engineering and Applications. Journal of Applied Physics, 112(9), 093703.

Shinagawa, T., Garcia-Esparza, A. T. and Takanabe, K. (2021). Electrodeposition Routes to Functional Oxide Thin Films. Electrochim. Acta, vol. 377, p. 138026.

Tlili, N., Nefzi, A., and Alhalaili, B. (2021). Structural, Optical, and Dielectric Properties of MgO Thin Films. Applied Physics A, 127(9), 723.

Zhang, Y., and Choi, K. (2019). Characterization of Tin-doped MgO Thin Films for Optoelectronic Applications," J. Mater. Chem. C, vol. 7, no. 44, pp. 13825–13833.